

# IDSelect: A RL-Based Cost-Aware Selection Agent for Video-based Multi-Modal Person Recognition

Yuyang Ji<sup>1</sup> Yixuan Shen<sup>1</sup> Kien Nguyen<sup>3</sup> Lifeng Zhou<sup>2</sup> Feng Liu<sup>1</sup>✉

<sup>1</sup> Department of Computer Science, Drexel University

<sup>2</sup> Department of Electrical and Computer Engineering, Drexel University

<sup>3</sup> School of Electrical Engineering and Robotics, Queensland University of Technology

## Abstract

Video-based person recognition achieves robust identification by integrating face, body, and gait. However, current systems waste computational resources by processing all modalities with fixed heavyweight ensembles regardless of input complexity. To address these limitations, we propose IDSelect, a reinforcement learning-based cost-aware selector that chooses one pre-trained model per modality per sequence to optimize the accuracy-efficiency trade-off. Our key insight is that an input-conditioned selector can discover complementary model choices that surpass fixed ensembles while using substantially fewer resources. IDSelect trains a lightweight agent end-to-end using actor-critic reinforcement learning with budget-aware optimization. The reward balances recognition accuracy with computational cost, while entropy regularization prevents premature convergence. At inference, the policy selects the most probable model per modality and fuses modality-specific similarities for the final score. Extensive experiments on challenging video-based datasets demonstrate IDSelect’s superior efficiency: on CCVID, it achieves 95.9% Rank-1 accuracy with 92.4% less computation than strong baselines while improving accuracy by 1.8%; on MEVID, it reduces computation by 41.3% while maintaining competitive performance. [Project](#)

## 1. Introduction

Whole-body person recognition [14, 17, 22, 23], integrating facial appearance, gait patterns, and body shape, has emerged as a robust approach for identifying individuals in unconstrained video environments. By fusing complementary biometric cues, these systems achieve superior accuracy in scenarios where single-modality methods fail (e.g., low-light or occluded conditions). Prior whole-body systems [14, 23] consistently demonstrate that these three cues

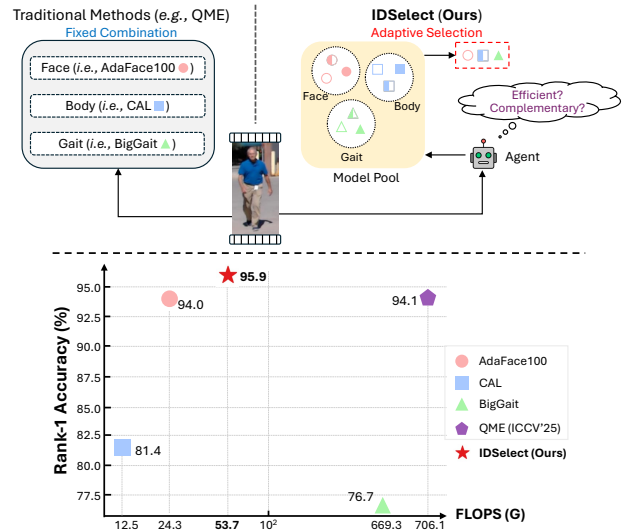


Figure 1. **Top:** Traditional multi-modal person recognition methods (e.g., QME [40]) use fixed model combinations for all inputs, while our IDSelect employs an RL-based cost-aware agent to adaptively select complementary models from diverse pools based on input characteristics. **Bottom:** Accuracy vs. computational cost on CCVID dataset [11]. Our method achieves superior accuracy (95.9%, +1.8%) with 92.4% fewer FLOPs than QME.

provide the strongest complementarity: faces are highly discriminative when resolution and pose are favorable, full-body appearance captures clothing and coarse shape, and gait remains reliable when faces are small, blurred, or occluded. This capability is crucial for applications in law enforcement, border security, surveillance, and public media analytics [9, 16, 39].

However, current state-of-the-art video-based multi-modal systems [23] are computationally impractical for real-world deployment: they typically use a *fixed combination* of heavy models for all modalities, incurring high memory and latency costs regardless of input difficulty. In resource-constrained settings like edge devices, processing every modality with large networks becomes prohibitively

✉ Corresponding author. f1397@drexel.edu

slow and power-intensive. This *one-size-fits-all* strategy ignores deployment budgets and fails to exploit the fact that not all inputs require powerful (and expensive) models.

Recent research has begun to expose these inefficiencies. The quality-guided fusion method [40], for instance, dynamically reweights modality contributions based on biometric sample quality, yielding accuracy gains under challenging conditions. However, such methods still assume a fixed pool of models and overlook the computational burden of always running multiple high-capacity networks. While some works [8, 21] have explored using lighter vs. heavier models within a single modality, such as creating lightweight face recognition architectures that reduce computational requirements, these approaches remain limited to single modality optimization and do not address the more complex challenge of joint optimization across modalities, *i.e.*, discovering which combination of face, gait, and body models achieves optimal accuracy-cost trade-offs. *A unified agent that dynamically adapts video-based multi-modal inference to varying computational budgets while discovering effective cross-modal synergies is highly desired.*

To address these limitations, we introduce **IDSelect**, an RL-based cost-aware agent that dynamically selects one pre-trained model per modality for each input. Our key insight is that a learned selection agent can discover complementary, input-conditioned model combinations that outperform static ensembles while utilizing significantly fewer computational resources. Importantly, we choose to select only one model per modality rather than multiple models within the same modality. This design choice is motivated by two key observations: First, models within the same modality tend to learn similar feature representations [15, 25], leading to high redundancy and diminishing marginal returns when combined. Second, true complementarity arises from *cross-modal* diversity; face, gait, and body capture fundamentally different biometric signatures—whereas selecting multiple face (or gait, or body) models primarily increases computational cost without proportional accuracy gains. By intelligently selecting model combinations based on input characteristics and budget constraints, IDSelect achieves competitive recognition performance at a significantly reduced computational cost.

Specifically, we first curate diverse pools of pre-trained models for each modality, spanning multiple architectures and training corpora to expose distinct cost–accuracy trade-offs. IDSelect employs a lightweight selection agent over a discrete video-based multi-modal action space, selecting *one model per modality* for each sample. During training, we construct positive/negative pairs and optimize an end-to-end hybrid objective that balances recognition accuracy, computational efficiency, and policy diversity. To make discrete selections learnable, we train the policy via an actor-critic reinforcement learning framework with a Lagrangian

budget controller, which enforces a target computation limit while balancing reward and cost. We also employ a budget curriculum that gradually tightens computational constraints to improve robustness across operating points. At inference, IDSelect adaptively determines optimal model combinations and aggregates per-modality similarities for final recognition. This mechanism enables IDSelect to discover effective model synergies while adapting computation to input characteristics.

In summary, the contributions of this work include:

- ◊ We propose **IDSelect**, an RL-based cost-aware agent that discovers complementary model combinations across face, gait, and body modalities for efficient whole-body recognition.

- ◊ We devise a lightweight selection agent trained end-to-end via an actor-critic reinforcement learning framework with a Lagrangian budget controller, enabling stable and budget-aware model selection.

- ◊ Extensive experiments on video-based whole-body datasets demonstrate that IDSelect discovers superior model combinations, achieving better accuracy-cost trade-offs than fixed and quality-guided fusion baselines.

## 2. Related work

**Whole-Body Person Recognition.** Video-based Multi-modal person recognition integrates complementary biometric traits—face, gait, and body shape—to achieve robust identification in challenging environments [14, 17, 22]. Unlike uni-modal approaches that rely on single biometric sources [5, 7, 11, 18], whole-body systems mitigate modality weaknesses through cross-modal complementarity. For instance, face recognition struggles with extreme pose variations; gait analysis is sensitive to clothing changes, and body shape can be affected by posture—yet their combination provides robustness where individual modalities fail. Recent advances have explored end-to-end pipelines integrating detection, restoration, and recognition [22, 23], demonstrating improved performance in unconstrained settings. However, these systems typically deploy all models simultaneously, leading to substantial computational overhead regardless of input complexity.

**Video-based Multi-Modal Biometric Fusion.** Traditional video-based multi-modal fusion relies on score-level strategies, where similarity scores from individual modalities are normalized and aggregated using simple operations [15]. More advanced methods adopt likelihood ratio-based fusion [25] for probabilistic interpretability or feature-level fusion [2] to capture cross-modal correlations. Recently, Zhu *et al.* [40] proposed the Quality-guided Mixture of score-fusion Experts (QME) framework, introducing pseudo-quality loss for quality estimation and score triplet loss for improved metric learning. The framework dynam-

ically weights modality contributions based on quality estimates, addressing cost-effectiveness by reducing overhead on poor-quality inputs. While the approach yields superior accuracy through quality-awareness, it fundamentally assumes *fixed* model pools and overlooks the burden of executing multiple heavyweight networks simultaneously.

**Adaptive and Cost-Aware Inference.** The computer vision community has developed sophisticated methods for input-dependent computation. Early-exit networks dynamically terminate inference when confidence thresholds are met. Teerapittayanon *et al.* [28] established the foundational BranchyNet framework for confidence-based early exits, while Yang *et al.* [32] demonstrated spatial redundancy exploitation via Resolution Adaptive Networks. Recent work on Adaptive Vision Transformers has pushed boundaries further: Yin *et al.* [34] developed A-ViT, achieving significant throughput improvements with minimal accuracy drop through adaptive token reduction, and Meng *et al.* [24] introduced fine-grained control over computational resources via learned usage policies. In video-based multi-modal settings, Panda *et al.* [26] proposed AdaMML for video understanding, achieving computational reduction through policies that adaptively select modality subsets. However, these adaptive approaches have not been systematically applied to multi-modal biometric recognition.

**Dynamic Model Selection.** Recent developments in efficient model design provide implementations of cost-aware architectures. George *et al.* [8] introduced EdgeFace, combining a CNN-Transformer hybrid architecture with Low Rank Linear modules, achieving exceptional results with minimal parameters. Yan *et al.* [31] demonstrated variable group convolutions for adaptive computational complexity in VarGFaceNet. In video-based multi-modal learning, He *et al.* [12] developed theoretical frameworks for quantifying modality utility using greedy submodular maximization, while recent work on Flex-MoE [36] addresses arbitrary modality combination with missing data robustness. However, existing methods either operate within single modalities or assume fixed model combinations, failing to discover complementary model synergies that could simultaneously improve accuracy and reduce computational cost. Reinforcement learning has also been explored for adaptive tool routing and dynamic inference [38], where an agent learns to select tools or sub-models based on inputs. Inspired by this line of work, our IDSelect agent addresses this gap by learning to discover optimal model combinations across face, gait, and body modalities through an actor-critic reinforcement learning policy that adaptively balances accuracy and computational cost.

## 3. Method

### 3.1. Preliminaries

Multi-modal person recognition leverages temporal sequences to extract complementary biometric traits for robust identification across diverse scenarios. Formally, let  $\mathcal{I}$  denote the set of all identities, and consider an input video sequence  $\mathbf{X} = \{x_1, x_2, \dots, x_T\}$  containing visual information from multiple biometric modalities  $\mathcal{M} = \{\text{face, gait, body}\}$  over  $T$  frames. Each modality provides a distinct temporal view: facial appearance captures identity-specific features across frames, gait patterns encode behavioral dynamics through walking motion, and body shape provides geometric cues that remain stable throughout the sequence. The video-based recognition pipeline operates in two phases: *enrollment* and *recognition*. During enrollment, gallery video sequences  $\mathcal{G} = \{\mathbf{X}_1^g, \mathbf{X}_2^g, \dots, \mathbf{X}_{|\mathcal{I}|}^g\}$  representing known identities are processed to extract representative temporal features. During recognition, a probe/query video  $\mathbf{X}^p$  is compared against the gallery through sequence-level similarity matching.

For each modality  $m \in \mathcal{M}$ , a temporal feature extractor  $f_m : \mathbb{R}^{T \times d_m} \rightarrow \mathbb{R}^{e_m}$  maps the modality-specific video sequence  $\mathbf{X}_m = \{x_{1,m}, x_{2,m}, \dots, x_{T,m}\}$  to a unified embedding space, where  $d_m$  represents the frame-level input dimensionality and  $e_m$  represents the final embedding dimension. The recognition process computes similarities between probe and gallery sequence embeddings:

$$s_m(\mathbf{X}^p, \mathbf{X}^g) = \frac{f_m(\mathbf{X}_m^p) \cdot f_m(\mathbf{X}_m^g)}{\|f_m(\mathbf{X}_m^p)\| \|f_m(\mathbf{X}_m^g)\|}. \quad (1)$$

Multi-modal fusion combines temporal evidence from all modalities to produce the final recognition score. Traditional approaches employ fixed strategies: score-level fusion through weighted averaging or feature-level fusion via joint embeddings; however, they struggle with varying input quality across modalities. Recent quality-guided methods like QME [40] address this through mixture-of-experts architectures that dynamically weight modalities based on estimated reliability, achieving superior performance by emphasizing high-quality inputs while downweighting degraded ones. However, these approaches assume *fixed* model availability and *presuppose that complementary information is accessible through pre-selected model combinations*, without addressing the computational overhead of executing all candidate networks, regardless of input complexity or deployment constraints.

### 3.2. IDSelect Architecture

We reformulate video-based person recognition as a *dynamic* resource allocation problem, where model combinations are discovered through learnable policies. The framework transforms the recognition pipeline from a static graph

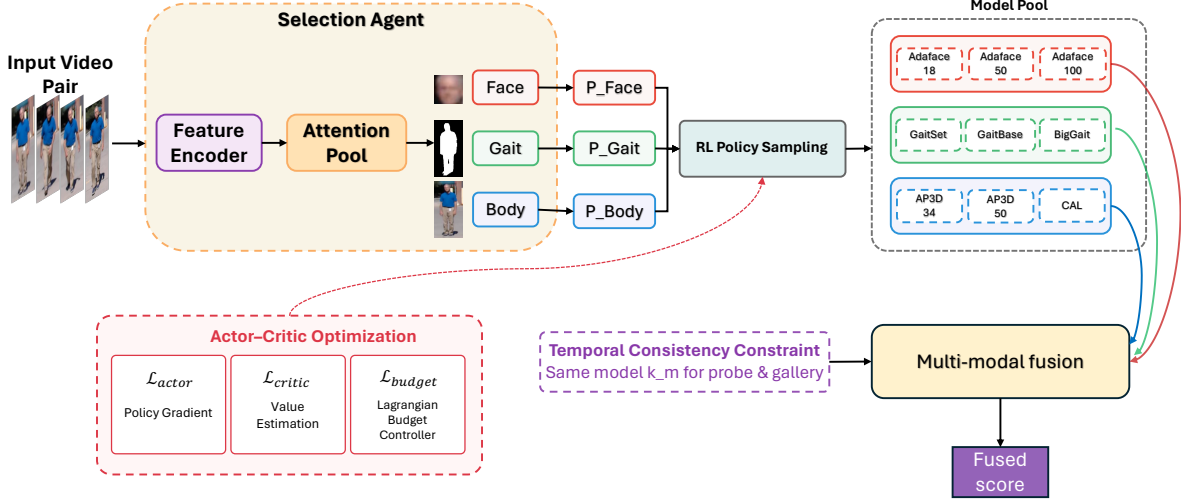


Figure 2. IDSelect framework architecture. The selection agent processes input video pairs through a feature encoder and attention pooling to generate modality-specific selection distributions. An actor-critic reinforcement learning policy optimizes model selection from pre-trained pools under a budget constraint. The framework minimizes a multi-objective loss combining classification reward, computational cost, and selection diversity to discover optimal model combinations for multi-modal fusion.

into an adaptive inference that balances recognition performance with computational efficiency.

The core innovation lies in decoupling model availability from model utilization. IDSelect introduces the hypothesis that different video sequences exhibit varying complexity patterns that can be effectively handled by different model combinations. This leads to a combinatorial optimization formulation where the selection agent  $\pi$  must solve:

$$\pi^*(\mathbf{X}) = \arg \max_{\pi} \left[ \sum_{m \in \mathcal{M}} \mathbb{E}[s_m(\mathbf{X}^p, \mathbf{X}^g | f_m^{\pi(m)})] - \mu \cdot \text{Cost}(\pi(\mathbf{X})) \right], \quad (2)$$

where  $f_m^{\pi(m)}$  represents the selected model for modality  $m$ , explicitly balancing recognition performance with computational cost to discover model synergies.

As illustrated in Fig. 2, IDSelect implements this using three interconnected components. The framework processes videos  $\mathbf{X}$  through a selection agent that analyzes cross-modal characteristics, applies reinforcement-driven selection mechanisms to choose model combinations, and ensures temporal coherence in feature extraction.

### 3.2.1. Input-Adaptive Selection Agent

The selection agent constructs a video-level representation by processing the entire video sequence:

$$h(\mathbf{X}) = \text{AttentionPool}(\{\phi_{\text{enc}}(x_t) : t = 1, 2, \dots, T\}), \quad (3)$$

where  $\phi_{\text{enc}}$  is a lightweight CNN encoder that extracts discriminative frame-level features optimized for model selec-

tion decisions, and AttentionPool learns to weight frames based on their informativeness for selection. This comprehensive temporal analysis captures sequence-level characteristics, including pose dynamics, motion complexity, visual quality variations, and modality-specific degradation patterns, enabling the agent to predict which model combinations will be most effective for the given input complexity. The resulting representation  $h(\mathbf{X})$  encodes both local frame-level properties and global sequence statistics necessary for informed model selection.

Modality-specific policy heads generate selection distributions:  $p_m = \text{Softmax}(\pi_{\theta}^m(h(\mathbf{X})))$ ,  $m \in \{\text{face, gait, body}\}$ . The key insight is that optimal model combinations exhibit complementary properties. When facial information is degraded, the policy compensates by selecting more sophisticated gait and body models, enabling the discovery of non-obvious model synergies.

### 3.2.2. RL-Guided Model Selection

IDSelect addresses the optimization challenge through a stochastic policy that is directly trained via reinforcement learning. During training, the face policy samples a single model index  $a_{\text{face}} \sim \text{Categorical}(p_{\text{face}})$ , while the body policy draws two actions without replacement by sequentially sampling from masked categorical distributions. The resulting action set  $\mathbf{a} = (a_{\text{face}}, a_{\text{body}}^{(1)}, a_{\text{body}}^{(2)})$  specifies one face model and two body models that will be executed for both probe and gallery clips. At inference time, selections become deterministic by choosing the argmax for the face branch and the top-2 logits for the body branch, ensuring a single forward pass per modality.

### 3.2.3. Complementary Feature Extraction.

IDSelect enforces temporal consistency through a constraint-preserving extraction strategy that addresses a critical challenge in adaptive model selection: ensuring that feature comparisons remain valid across different model choices. The framework requires that the same selected model be applied to both probe and gallery sequences to maintain embedding compatibility:

$$\tilde{\mathbf{z}}_m^p = f_m^{k_m}(\mathbf{X}_m^p), \quad \tilde{\mathbf{z}}_m^g = f_m^{k_m}(\mathbf{X}_m^g), \quad (4)$$

where  $k_m$  is the index chosen by the policy for modality  $m$ , at inference we use  $k_m = \arg \max_j p_m^j$ .

This consistency constraint is essential because different models  $f_m^i$  and  $f_m^j$  typically produce embeddings in different feature spaces, making direct comparison meaningless. By ensuring that probe and gallery features are extracted using identical models, IDSelect maintains the validity of the cosine similarity computation:

$$s_m = \cos(\tilde{\mathbf{z}}_m^p, \tilde{\mathbf{z}}_m^g) = \frac{\tilde{\mathbf{z}}_m^p \cdot \tilde{\mathbf{z}}_m^g}{\|\tilde{\mathbf{z}}_m^p\| \|\tilde{\mathbf{z}}_m^g\|}. \quad (5)$$

Furthermore, within each video sequence, the selected model processes all frames consistently to preserve temporal coherence. This design choice ensures that the temporal modeling capabilities of gait recognition models remain intact while enabling adaptive selection at the sequence level.

The final recognition score aggregates evidence across all modalities through simple averaging:  $s_{\text{final}} = \frac{1}{|\mathcal{M}|} \sum_{m \in \mathcal{M}} s_m$ . This aggregation strategy, while simple, proves effective in practice as the selection mechanism automatically balances contribution of modalities by choosing appropriate model complexities rather than relying on learned fusion weights.

### 3.3. Model Training

IDSelect is trained end-to-end through an actor-critic formulation that optimizes a reward balancing recognition accuracy against normalized computational cost. Let  $s_{\text{final}}$  denote the fused similarity for a paired sample with the ground-truth label  $y \in \{0, 1\}$ . The reward for action set  $\mathbf{a}$  is defined as

$$r = 1 - \underbrace{\text{BCE}(\sigma(s_{\text{final}}), y)}_{\text{utility}} - \lambda \underbrace{C(\mathbf{a})}_{\text{cost}}, \quad (6)$$

where  $\sigma(\cdot)$  is the sigmoid function, BCE denotes binary cross-entropy, and  $C(\mathbf{a})$  is the average of modality-specific FLOP costs normalized by their modality maxima. The scalar  $\lambda$  is a Lagrange multiplier that self-adjusts to satisfy the target budget  $C_{\text{target}}$ : after each batch, we update  $\lambda \leftarrow \max(0, \lambda + \eta(\bar{C} - C_{\text{target}}))$ , where  $\bar{C}$  is the observed batch-average cost and  $\eta$  is a small step size.

A value head  $V_\psi(h(\mathbf{X}))$  predicts the expected reward to stabilize policy learning. The actor loss combines policy gradients with entropy regularization:

$$\mathcal{L}_{\text{actor}} = -(r - V_\psi) \cdot \log \pi_\theta(\mathbf{a} | \mathbf{X}) - \beta \mathcal{H}(\pi_\theta), \quad (7)$$

where  $\mathcal{H}$  denotes the entropy of the joint action distribution, and  $\beta$  encourages exploration early in training. The critic learns by minimizing  $\mathcal{L}_{\text{critic}} = (r - V_\psi)^2$ , and the training objective is  $\mathcal{L}_{\text{actor}} + \alpha \mathcal{L}_{\text{critic}}$  with  $\alpha$  controlling the critic weight. All biometric backbones remain frozen, so gradients only update the selection agent, the value head, and the optimizer state for the Lagrange multiplier.

### 3.4. Implementation Details

We implement the selection agent with a lightweight CNN encoder featuring five convolutional layers (3→64→128→256→512 channels), followed by adaptive pooling and projection to 512-dimensional features. Modality-specific agent heads are implemented as 3-layer MLPs (512→256→128 dimensions) that output selection logits for each modality’s available models. Reinforcement learning uses the Adam optimizer with learning rate  $5 \times 10^{-4}$ , batch size 8, and weight decay  $1 \times 10^{-4}$ . We apply gradient clipping with max norm 1.0, entropy coefficient  $\beta = 0.01$ , critic weight  $\alpha = 0.5$ , and target normalized cost  $C_{\text{target}} = 0.45$ . The Lagrange multiplier is initialized at 0.1 and updated with step size  $5 \times 10^{-3}$ . All pre-trained models remain frozen, focusing optimization on agent learning only. During training, we sample video pairs  $(\mathbf{X}^p, \mathbf{X}^g)$  with positive and negative identity labels. The selection agent analyzes each query video  $\mathbf{X}^p$  to determine model selections, which are applied to both query and gallery videos for feature extraction.

## 4. Experiments

### 4.1. Experimental Setup

**Datasets.** Following the setting of QME [40], we evaluate IDSelect on two challenging video-based person recognition datasets that exhibit significant real-world variations. CCVID dataset [11] contains 2,856 sequences across 226 identities, where each identity has 2 to 5 different suits of clothing. The dataset presents challenging variations, including different clothing across sessions, varying illumination conditions, and temporal gaps between captures. MEVID dataset [4] spans extensive indoor and outdoor environments across nine unique dates in a 73-day window, featuring 158 unique people wearing 598 outfits taken from 8,092 tracklets, with an average length of 590 frames captured from 33 camera views. The dataset emphasizes richer information per individual, with 4 outfits per identity and 33 viewpoints across 17 locations, inherited from the MEVA

person activities dataset, which is intentionally demographically balanced.

**Model Pools.** We strategically design diverse model pools to evaluate IDSelect’s adaptability across different computational constraints and model capabilities. For CCVID, we evaluate two complementary configurations:

- *Configuration 1 (QME Baseline Comparison):* This configuration directly compares against the QME [40] (ICCV’25) baseline by including the *exact same* heavyweight models as the most expensive options per modality: AdaFace101 [18] (ResNet101 backbone, face), CAL (ResNet50, body), and BigGait (ViT-B16, gait). We additionally include lighter alternatives across all modalities: AdaFace18/50 (ResNet18/50 backbones) for face recognition, AP3D 34/50 [10] (ResNet34/50 backbones) for body analysis, and GaitSet [3]/GaitBase [7] for gait recognition. This design enables fair comparison with QME while demonstrating IDSelect’s ability to achieve superior efficiency through intelligent model selection rather than brute-force heavyweight fusion.
- *Configuration 2 (SOTA Model Diversity):* To validate generalization beyond QME’s specific model choices, we incorporate diverse state-of-the-art architectures, including TF-CLIP [35] for body recognition and DeepGaitv2 for gait analysis, alongside AdaFace variants and complementary models (CAL [11], AP3D 50 [10], GaitSet [3], GaitBase [7]). This configuration tests IDSelect’s adaptability to different SOTA architectures while maintaining reasonable computational constraints.

For MEVID’s challenging conditions, following the setting of QME [40], we focus on face-body fusion using AdaFace variants (AdaFace18/50/101 with ResNet18/50/101 backbones) and five body models: CAL [11], AGRL [30], Attn-CL [27], AP3D 50 [10], and PiT [37]. This configuration excludes gait modality due to severely degraded body image resolution, which prevents reliable gait silhouette extraction.

**Baselines.** We compare against comprehensive baseline categories: (1) Single-modality approaches using individual face, gait, and body models, including BigGait [33], which we use with weights trained on the CCPG long-range video dataset [20]; (2) Advanced fixed fusion techniques such as Asym-AOI [13], BSSF [29], and Farsight [22]; (3) Universal multi-modal models, including SapiensID [19], a unified face–body model pre-trained on the WebBody4M dataset [19]; and (4) Quality-guided methods, including QME [40] (ICCV’25).

**Evaluation Metrics.** Following standard person re-identification protocols, we report Rank-1 accuracy and mean Average Precision (mAP) on fixed test sets. For computational efficiency analysis, we measure GFLOPs based on the model architecture and input size.

Table 1. Performance comparison on CCVID *Configuration 1*. IDSelect achieves superior accuracy-efficiency trade-offs compared to single modality baselines, fixed fusion strategies, and quality-guided methods. ‘Ada.’ denotes input-adaptive selection. Colored icons in “Comb.” represent modality and model capacity (○=face, □=body, △=gait; fill level increases with model size, from light to heavy). Models marked with an asterisk \* are not finetuned on the CCVID dataset, while all other models are finetuned.

| Method                     | Arch.     | GFLOPs↓     | Comb. | Rank1↑      | mAP↑        |
|----------------------------|-----------|-------------|-------|-------------|-------------|
| <b>Face Models</b>         |           |             |       |             |             |
| AdaFace18* [18]            | R18       | 5.2         | ○     | 90.5        | 80.4        |
| AdaFace50* [18]            | R50       | 12.7        | ●     | 91.7        | 82.9        |
| AdaFace101* [18]           | R101      | 24.3        | ●     | 94.0        | 87.9        |
| <b>Body Models</b>         |           |             |       |             |             |
| AP3D 34 [10]               | R34       | 7.6         | □     | 75.1        | 73.6        |
| AP3D 50 [10]               | R50       | 8.5         | ■     | 80.9        | 79.2        |
| CAL [11]                   | R50       | 12.5        | ■     | 81.4        | 74.7        |
| <b>Gait Models</b>         |           |             |       |             |             |
| GaitSet [3]                | CNN-6     | 6.5         | △     | 79.3        | 73.8        |
| GaitBase [7]               | R9        | 71.0        | △     | 64.0        | 61.4        |
| BigGait* [33]              | DINOv2-S* | 669.3       | ▲     | 76.7        | 61.0        |
| <b>Weighted-sum Fusion</b> |           |             |       |             |             |
| Face + Gait Max            | –         | 693.6       | ●▲    | 91.4        | 85.7        |
| Face + Gait Min            | –         | 11.7        | ○△    | 94.4        | 91.7        |
| Face + Body Max            | –         | 36.8        | ●■    | 93.6        | 90.0        |
| Face + Body Min            | –         | 12.8        | ○□    | 92.2        | 86.6        |
| Gait + Body Max            | –         | 681.8       | ▲■    | 84.2        | 78.7        |
| Gait + Body Min            | –         | 14.1        | △□    | 89.2        | 86.3        |
| Face + Body + Gait Max     | –         | 706.1       | ●■▲   | 91.7        | 88.9        |
| Face + Body + Gait Min     | –         | 19.4        | ○□△   | 94.5        | 93.5        |
| Asym-AOI [13]              | –         | 706.1       | ●□△   | 92.3        | 90.0        |
| BSSF [29]                  | –         | 706.1       | ●□△   | 91.8        | 91.1        |
| SapiensID* [19]            | ViT-Base  | –           | –     | 92.6        | 77.8        |
| Farsight [22]              | –         | 706.1       | ●□△   | 92.9        | 91.2        |
| QME (ICCV’25, [40])        | –         | 706.1       | ●□△   | 92.6        | 91.6        |
| QME (ICCV’25, [40])        | –         | 706.1       | ●□△   | 94.1        | 90.8        |
| <b>IDSelect</b>            | –         | <b>53.7</b> | Ada.  | <b>95.9</b> | <b>94.6</b> |

## 4.2. Results on CCVID Dataset

Tab. 1 presents results on CCVID *Configuration 1*, where IDSelect demonstrates exceptional efficiency gains while improving accuracy. IDSelect achieves 95.9% Rank-1 and 94.6% mAP while consuming only 53.7 GFLOPs—a 92.4% reduction compared to QME’s 706.1 GFLOPs with +1.8% higher accuracy. This dramatic computational saving demonstrates that adaptive model selection can discover superior model combinations that heavyweight exhaustive fusion approaches fail to find.

Tab. 2 shows results on CCVID *Configuration 2* with a more computationally constrained model pool. IDSelect maintains strong performance with 97.4% Rank-1 and 92.7% mAP at 54.8 GFLOPs, achieving 2.2× computational savings compared to exhaustive Max fusion. Notably, *Configuration 2* achieves higher accuracy than *Configuration 1* (97.4% vs 95.9% Rank-1) despite operating within tighter computational constraints, demonstrating IDSelect’s adaptability to different model pool characteristics while maintaining consistent efficiency.

IDSelect consistently outperforms fixed fusion strategies across varying computational budgets, demonstrating that

Table 2. Performance comparison on CCVID *Configuration 2*. IDSelect demonstrates adaptability across model pool configurations, maintaining strong performance while achieving significant computational savings compared to exhaustive fusion.

| Method             | Arch.   | GFLOPs↓     | Comb. | Rank1↑      | mAP↑        |
|--------------------|---------|-------------|-------|-------------|-------------|
| <b>Face Models</b> |         |             |       |             |             |
| AdaFace18* [18]    | R18     | 5.2         | ○     | 90.5        | 80.4        |
| AdaFace50* [18]    | R50     | 12.7        | ◐     | 91.7        | 82.9        |
| AdaFace101* [18]   | R101    | 24.3        | ◑     | 94.0        | 87.9        |
| <b>Body Models</b> |         |             |       |             |             |
| AP3D 50 [10]       | R50     | 8.5         | □     | 80.9        | 79.2        |
| CAL [11]           | R50     | 12.5        | ◻     | 81.4        | 74.7        |
| TF CLIP [35]       | ViT-B16 | 14.8        | ■     | 90.8        | 90.4        |
| <b>Gait Models</b> |         |             |       |             |             |
| GaitSet [3]        | CNN-6   | 6.5         | △     | 79.3        | 73.8        |
| GaitBase [7]       | R9      | 71.0        | ▲     | 64.0        | 61.4        |
| DeepGaitv2 [6]     | P3D-R*  | 83.5        | ▲     | 68.5        | 59.9        |
| IDSelect (w/o RL)  | –       | 54.8        | Ada.  | 94.8        | 92.5        |
| IDSelect (Conf1)   | –       | <b>53.7</b> | Ada.  | 95.9        | <b>94.6</b> |
| IDSelect (Conf2)   | –       | 54.8        | Ada.  | <b>97.4</b> | 92.7        |

Table 3. Performance comparison on MEVID dataset with face-body fusion configurations. Results highlight the benefits of cross-modal complementarity while revealing diminishing returns from intra-modal redundancy among body models.

| Method                              | Arch.   | GFLOPs↓     | Comb. | Rank1↑      | mAP↑        |
|-------------------------------------|---------|-------------|-------|-------------|-------------|
| <b>Face Models</b>                  |         |             |       |             |             |
| AdaFace18* [18]                     | R18     | 5.2         | ○     | 18.4        | 7.7         |
| AdaFace50* [18]                     | R50     | 12.7        | ◐     | 23.1        | 9.1         |
| AdaFace101* [18]                    | R101    | 24.3        | ◑     | 25.0        | 8.1         |
| <b>Body Models</b>                  |         |             |       |             |             |
| AP3D [10]                           | R50     | 8.5         | □     | 35.4        | 14.6        |
| CAL [11]                            | R50     | 12.5        | ◻     | 52.5        | 27.1        |
| Attn-CL [27]                        | R50     | 12.7        | ◻     | 44.0        | 16.1        |
| PiT [37]                            | ViT-B16 | 22.6        | ■     | 34.2        | 13.6        |
| AGRL [30]                           | R50     | 48.2        | ■     | 51.9        | 25.5        |
| <b>1 face model + 1 body model</b>  |         |             |       |             |             |
| GEFF [1]                            | –       | 36.8        | ◐◻    | 32.9        | 18.8        |
| QME [40]                            | –       | 36.8        | ◑◻    | 33.5        | 19.9        |
| IDSelect                            | –       | <b>28.7</b> | Ada.  | <b>50.0</b> | <b>21.5</b> |
| <b>1 face model + 2 body models</b> |         |             |       |             |             |
| Asym-AO1 [13]                       | –       | 85.0        | ◑◻◻   | 52.5        | 22.9        |
| BSSF [29]                           | –       | 85.0        | ◑◻◻   | 53.5        | 27.4        |
| Farsight [22]                       | –       | 85.0        | ◑◻◻   | 53.8        | 25.4        |
| QME (ICCV’25, [40])                 | –       | 85.0        | ◑◻◻   | 55.7        | <b>28.2</b> |
| IDSelect                            | –       | <b>49.9</b> | Ada.  | <b>56.0</b> | 24.4        |

adaptive selection discovers superior trade-offs unavailable to static approaches. Compared to QME [40], IDSelect maintains superior efficiency while achieving competitive or improved accuracy, demonstrating that learned selection agents can effectively exploit *cross-modal complementarity* to optimize accuracy-efficiency trade-offs without compromising recognition performance.

### 4.3. Results on MEVID Dataset

Tab. 3 presents results on the challenging MEVID dataset with face-body fusion configurations. Following QME’s ex-

Table 4. Modality combination analysis on CCVID *Configuration 1*. Results demonstrate the effectiveness of cross-modal complementarity, with the full three-modality approach achieving optimal performance while two-modality combinations provide competitive accuracy at reduced computational cost.

| Method      | GFLOPs↓ | Rank1↑ | mAP↑ |
|-------------|---------|--------|------|
| Face + Gait | 46.1    | 95.5   | 91.2 |
| Face + Body | 31.4    | 94.2   | 90.3 |
| Gait + Body | 29.9    | 87.5   | 85.1 |
| all         | 53.7    | 95.9   | 94.6 |

perimental setup, we evaluate configurations with varying model pool sizes to demonstrate IDSelect’s effectiveness under extreme viewing conditions. For the **1 face + 1 body model** configuration, IDSelect achieves 50.0% Rank-1 and 21.5% mAP at 28.7 GFLOPs. Notably, this is lower than the best single body model (52.5% Rank-1), indicating that under MEVID’s extreme viewing conditions, the degraded face modality (25.0% Rank-1) actually reduces overall performance when fused with body features. In the **1 face + 2 body models** configuration, IDSelect reaches 56.0% Rank-1 and 24.4% mAP at 49.9 GFLOPs, outperforming QME’s 55.7% while achieving 1.7× computational savings.

The results reveal that under extreme surveillance conditions, face information can be too degraded to provide complementary benefits. However, the modest improvement when expanding from 1 to 2 body models (56.0% vs 50.0% Rank-1) suggests significant overlap among the body models, making it challenging to identify truly complementary combinations within the same modality. This finding validates IDSelect’s design principle that optimal model selection benefits most from cross-modal diversity rather than intra-modal redundancy. Future work should explore face + gait + body fusion on datasets where all three modalities are reliable, as combining fundamentally different biometric cues offers the greatest complementarity potential.

### 4.4. Analysis and Discussion

**Modality Complementarity and Selection Patterns.** To understand how IDSelect discovers complementary model combinations, we analyze performance across modality combinations and examine the learned selection patterns. Tab. 4 reveals that cross-modal fusion consistently outperforms individual modalities, with the most significant gains occurring when combining fundamentally different biometric cues. Face + Gait achieves 95.5% Rank-1, demonstrating strong complementarity between facial features and temporal gait patterns. Face + Body fusion achieves 94.2% Rank-1, showing efficient performance when gait analysis is unavailable. Gait + Body achieves 87.5% Rank-1, indicating that body shape and gait dynamics provide reasonable recognition even without facial information. The three-

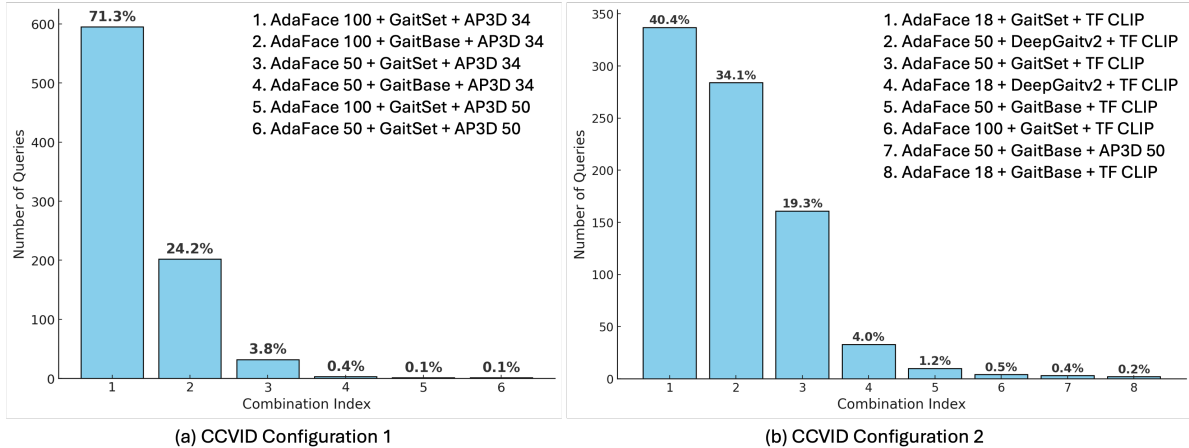


Figure 3. Model selection frequency distribution for CCVID configurations. (a) *Configuration 1* shows concentrated patterns with IDSelect predominantly selecting `adaface_101 + gaitset + ap3d_34` (71.3%) and `adaface_101 + gaitbase + ap3d_34` (24.2%). (b) *Configuration 2* exhibits more diverse selection patterns, demonstrating adaptability to different model pool characteristics.



Figure 4. Adaptive model selection examples on CCVID. The agent uses lighter models for clear inputs and switches to stronger models for challenging or low-quality cases.

modality approach achieves optimal performance (95.9% Rank-1, 94.6% mAP), where the significant mAP improvement justifies the additional computational cost. Fig. 3 reveals the learned selection patterns. In *Configuration 1*, IDSelect exhibits concentrated preferences, selecting `adaface_101 + gaitset + ap3d_34` in 71.3% of cases, indicating that the agent prioritizes the most accurate face model while adaptively choosing gait models based on input characteristics. *Configuration 2* shows more diverse selections, demonstrating the framework’s adaptability to model-pool characteristics.

**Efficiency Trade-offs.** IDSelect consistently discovers optimal efficiency regions that are unavailable to fixed strategies. As shown in Tabs. 1 and 2, while Min” combinations achieve reasonable efficiency but lower accuracy (Face + Body + Gait Min: 94.5–95.1% Rank-1 at 19.4–20.2 GFLOPs), Max” combinations provide varying accuracy at a high computational cost (Tab. 1: Face + Body + Gait Max achieves 91.7% Rank-1 at 706.1 GFLOPs). IDSelect finds

superior trade-offs with 95.9–97.4% Rank-1 accuracy at a moderate cost (53.7–54.8 GFLOPs). The method achieves substantial savings: a 13.2× reduction on *Configuration 1* while improving accuracy from 94.1% to 95.9%; a 2.2× reduction on *Configuration 2*; and a 1.7× savings on MEVID while maintaining competitive performance.

**Limitations.** IDSelect requires curating diverse model pools, incurring upfront costs not captured in inference metrics. However, this one-time investment becomes more practical as the community releases abundant pre-trained models (e.g., AdaFace, BigGait, SapiensID) that can be reused, turning pool construction into curation rather than training. While the framework must keep multiple models in memory, this overhead is acceptable in most scenarios where computational savings outweigh storage, and edge devices now support larger model capacities. Additionally, our experiments with small pools (3–5 models per modality) open opportunities to study scalability to larger ecosystems and domain adaptation of selection policies across deployments. Future work includes hierarchical selection strategies and backup mechanisms for cases where individual modalities fail under severe degradation.

## 5. Conclusion

We introduced **IDSelect**, an RL-based cost-aware agent that transforms video-based person recognition from static heavyweight fusion into adaptive resource allocation, achieving up to 92.4% computational reduction while improving accuracy. The key insight is that learned selection policies uncover complementary cross-modal synergies that fixed approaches cannot, especially the finding that diversity across face, gait, and body yields greater gains than intra-modal redundancy. By balancing recognition perfor-

mance and computational cost through input-conditioned model selection, IDSelect enables the practical deployment of multi-modal video biometrics in resource-constrained settings, shifting the paradigm from “use everything available” to “select only what is needed.”

## References

- [1] Daniel Arkushin, Bar Cohen, Shmuel Peleg, and Ohad Fried. Geff: Improving any clothes-changing person reid model using gallery enrichment with face features. In *WACV*, 2024. 7
- [2] Hsu Mon Lei Aung, Charnchai Pluemtiwiriyaewej, Kazuhiko Hamamoto, and Somkiat Wangsiripitak. Multimodal biometrics recognition using a deep convolutional neural network with transfer learning in surveillance videos. *Computation*, 2022. 2
- [3] Hanqing Chao, Kun Wang, Yiwei He, Junping Zhang, and Jianfeng Feng. Gaitset: Cross-view gait recognition through utilizing gait as a deep set. *TPAMI*, 2021. 6, 7
- [4] Daniel Davila, Dawei Du, Bryon Lewis, Christopher Funk, Joseph Van Pelt, Roderic Collins, Kellie Corona, Matt Brown, Scott McCloskey, Anthony Hoogs, et al. Mevid: Multi-view extended videos with identities for video person re-identification. In *WACV*, 2023. 5
- [5] Jiankang Deng, Jia Guo, Niannan Xue, and Stefanos Zafeiriou. Arcface: Additive angular margin loss for deep face recognition. In *CVPR*, 2019. 2
- [6] Chao Fan, Saihui Hou, Yongzhen Huang, and Shiqi Yu. Exploring deep models for practical gait recognition. *arXiv preprint arXiv:2303.03301*, 2023. 7
- [7] Chao Fan, Junhao Liang, Chuanfu Shen, Saihui Hou, Yongzhen Huang, and Shiqi Yu. Opengait: Revisiting gait recognition towards better practicality. In *CVPR*, 2023. 2, 6, 7
- [8] Anjith George, Christophe Ecabert, Hatef Otroushi Shahreza, Ketan Kotwal, and Sébastien Marcel. Edgeface: Efficient face recognition model for edge devices. *T-BIOM*, 2024. 2, 3
- [9] Shaogang Gong and Tao Xiang. Person re-identification. In *Visual Analysis of Behaviour: From Pixels to Semantics*. Springer London, 2011. 1
- [10] Xinqian Gu, Hong Chang, Bingpeng Ma, Hongkai Zhang, and Xilin Chen. Appearance-preserving 3d convolution for video-based person re-identification. In *ECCV*, 2020. 6, 7
- [11] Xinqian Gu, Hong Chang, Bingpeng Ma, Shutao Bai, Shiguang Shan, and Xilin Chen. Clothes-changing person re-identification with rgb modality only. In *CVPR*, 2022. 1, 2, 5, 6, 7
- [12] Yifei He, Runxiang Cheng, Gargi Balasubramaniam, Yao-Hung Hubert Tsai, and Han Zhao. Efficient modality selection in multimodal learning. *JMLR*, 2024. 3
- [13] Abderrahmane Herbadji, Zahid Akhtar, Kamran Siddique, Noubel Guermat, Lahcene Ziet, Mohamed Cheniti, and Khan Muhammad. Combining multiple biometric traits using asymmetric aggregation operators for improved person recognition. *Symmetry*, 2020. 6, 7
- [14] Siyuan Huang, Ram Prabhakar Kathirvel, Yuxiang Guo, Chun Pong Lau, and Rama Chellappa. Whole-body detection, identification and recognition at altitude and range. *T-BIOM*, 2024. 1, 2
- [15] Anil Jain, Karthik Nandakumar, and Arun Ross. Score normalization in multimodal biometric systems. *Pattern recognition*, 2005. 2
- [16] Anil K. Jain, Arun A. Ross, Karthik Nandakumar, and Thomas Swearingen. *Introduction to Biometrics*. Springer Cham, 2 edition, 2025. 1
- [17] Bhavin Jawade, Deen Dayal Mohan, Prajwal Shetty, Dennis Fedorishin, Srirangaraj Setlur, and Venu Govindaraju. Conan: Conditional neural aggregation network for unconstrained long range biometric feature fusion. *T-BIOM*, 2024. 1, 2
- [18] Minchul Kim, Anil K Jain, and Xiaoming Liu. Adaface: Quality adaptive margin for face recognition. In *CVPR*, 2022. 2, 6, 7
- [19] Minchul Kim, Dingqiang Ye, Yiyang Su, Feng Liu, and Xiaoming Liu. Sapiensid: Foundation for human recognition. In *CVPR*, 2025. 6
- [20] Weijia Li, Saihui Hou, Chunjie Zhang, Chunshui Cao, Xu Liu, Yongzhen Huang, and Yao Zhao. An in-depth exploration of person re-identification and gait recognition in cloth-changing conditions. In *CVPR*, 2023. 6
- [21] Xianyang Li, Feng Wang, Qinghao Hu, and Cong Leng. Airface: Lightweight and efficient model for face recognition. In *ICCVW*, 2019. 2
- [22] Feng Liu, Ryan Ashbaugh, Nicholas Chimitt, Najmul Hassan, Ali Hassani, Ajay Jaiswal, Minchul Kim, Zhiyuan Mao, Christopher Perry, Zhiyuan Ren, et al. Farsight: A physics-driven whole-body biometric system at large distance and altitude. In *WACV*, 2024. 1, 2, 6, 7
- [23] Feng Liu, Nicholas Chimitt, Lanqing Guo, Jitesh Jain, Aditya Kane, Minchul Kim, Wes Robbins, Yiyang Su, Dingqiang Ye, Xingguang Zhang, et al. Person recognition at altitude and range: Fusion of face, body shape and gait. *arXiv preprint arXiv:2505.04616*, 2025. 1, 2
- [24] Lingchen Meng, Hengduo Li, Bor-Chun Chen, Shiyi Lan, Zuxuan Wu, Yu-Gang Jiang, and Ser-Nam Lim. Adavit: Adaptive vision transformers for efficient image recognition. In *CVPR*, 2022. 3
- [25] Karthik Nandakumar, Yi Chen, Sarat C Dass, and Anil Jain. Likelihood ratio-based biometric score fusion. *TPAMI*, 2008. 2
- [26] Rameswar Panda, Chun-Fu Richard Chen, Quanfu Fan, Ximeng Sun, Kate Saenko, Aude Oliva, and Rogerio Feris. Adamml: Adaptive multi-modal learning for efficient video recognition. In *ICCV*, 2021. 3
- [27] Priyank Pathak, Amir Erfan Eshratifar, and Michael Gormish. Video person re-id: Fantastic techniques and where to find them (student abstract). In *AAAI*, 2020. 6, 7
- [28] Surat Teerapittayanon, Bradley McDanel, and Hsiang-Tsung Kung. Branchynet: Fast inference via early exiting from deep neural networks. In *ICPR*, 2016. 3

- [29] Jackson Horlick Teng, Thian Song Ong, Tee Connie, Kalaiarasi Sonai Muthu Anbananthen, and Pa Pa Min. Optimized score level fusion for multi-instance finger vein recognition. *Algorithms*, 2022. [6](#), [7](#)
- [30] Yiming Wu, Omar El Farouk Bourahla, Xi Li, Fei Wu, Qi Tian, and Xue Zhou. Adaptive graph representation learning for video person re-identification. *IEEE TIP*, 2020. [6](#), [7](#)
- [31] Mengjia Yan, Mengao Zhao, Zining Xu, Qian Zhang, Guoli Wang, and Zhizhong Su. Vargfacenet: An efficient variable group convolutional neural network for lightweight face recognition. In *ICCVW*, 2019. [3](#)
- [32] Le Yang, Yizeng Han, Xi Chen, Shiji Song, Jifeng Dai, and Gao Huang. Resolution adaptive networks for efficient inference. In *CVPR*, 2020. [3](#)
- [33] Dingqiang Ye, Chao Fan, Jingzhe Ma, Xiaoming Liu, and Shiqi Yu. Biggait: Learning gait representation you want by large vision models. In *CVPR*, 2024. [6](#)
- [34] Hongxu Yin, Arash Vahdat, Jose M Alvarez, Arun Mallya, Jan Kautz, and Pavlo Molchanov. A-vit: Adaptive tokens for efficient vision transformer. In *CVPR*, 2022. [3](#)
- [35] Chenyang Yu, Xuehu Liu, Yingquan Wang, Pingping Zhang, and Huchuan Lu. Tf-clip: Learning text-free clip for video-based person re-identification. In *AAAI*, 2024. [6](#), [7](#)
- [36] Sukwon Yun, Inyoung Choi, Jie Peng, Yangfan Wu, Jingxuan Bao, Qiyiwen Zhang, Jiayi Xin, Qi Long, and Tianlong Chen. Flex-moe: Modeling arbitrary modality combination via the flexible mixture-of-experts. In *NeurIPS*, 2024. [3](#)
- [37] Xianghao Zang, Ge Li, and Wei Gao. Multidirection and multiscale pyramid in transformer for video-based pedestrian retrieval. *IEEE TII*, 2022. [6](#), [7](#)
- [38] Haozhen Zhang, Tao Feng, and Jiakuan You. Router-r1: Teaching llms multi-round routing and aggregation via reinforcement learning. In *NeurIPS*, 2025. [3](#)
- [39] Liang Zheng, Yi Yang, and Alexander G Hauptmann. Person re-identification: Past, present and future. *arXiv preprint arXiv:1610.02984*, 2016. [1](#)
- [40] Jie Zhu, Yiyang Su, Minchul Kim, Anil Jain, and Xiaoming Liu. A quality-guided mixture of score-fusion experts framework for human recognition. In *ICCV*, 2025. [1](#), [2](#), [3](#), [5](#), [6](#), [7](#)